Optics Communications 335 (2015) 140–145

Contents lists available at ScienceDirect

Optics Communications

journal homepage: www.elsevier.com/locate/optcom

Surface defect lattice solitons in photovoltaic-photorefractive crystals

Chunxiang Wang, Keqing Lu*, Weijun Chen, Huimin Yu, Kai Hu

School of Electronics and Information Engineering, Tianjin Polytechnic University, Tianjin 300387, China

ARTICLE INFO

Article history:
Received 30 July 2014
Received in revised form
2 September 2014
Accepted 5 September 2014
Available online 18 September 2014

Keywords:
Surface solitons
Photonic lattices
Defect strength
Nonlinear optics

ABSTRACT

We report that surface defect lattice solitons (SDLSs) can be supported at the interface between the photonic lattices with a defect and the uniform photovoltaic-photorefractive (PP) crystal. We show that these SDLSs exist only in the semi-infinite gap when the defect is positive and both in the semi-infinite gap and the first gap when the defect is negative. For a positive defect, SDLSs are stable in the high and low power regions and unstable in the moderate power region. For a negative defect, SDLSs in the semi-infinite gap are stable in the moderate power region and unstable in the high and low power regions. In the first gap, SDLSs are stable in the all power regions. We find that the stable region of SDLSs increases with the positive defect strength and decreases with an increase in the negative defect strength and the power of SDLSs decrease with an increase in the positive defect strength and increase with the negative defect strength.

1. Introduction

Light propagation in periodic optical systems such as waveguide arrays, photonic crystals, and optically-induced photonic lattices has attracted substantial research interest due to its physics and light-routing applications. In such periodic systems, linear light propagation exhibits Bloch bands and forbidden bandgaps. Gap solitons can exist in different bandgaps and form by the nonlinear coupling between forward- and backward-propagating waves when both experience Bragg scattering from the periodic structures. To date, a wide variety of gap solitons in different gaps are known: fundamental solitons [1–7], dipole solitons [8,9], vortex solitons [10–12], quadrupole solitons [13], and defect solitons [14–19], all of which form in bulk periodic mediums. Gap solitons may also exist at periodically modulated surfaces [20]. Surface solitons at the interface between the uniform media and the periodic waveguide arrays [21–26], at the interface of two periodic media [27–30], and at the interface between the photonic lattices and the uniform photorefractive crystals [31,32] have been proposed and observed. On the other hand, the interface with a defect can support surface solitons [33,34]. Surface defect lattice solitons (SDLSs) in biased non-photovoltaic-photorefractive crystals have been predicted [35]. Therefore, it would be of interest to explore whether SDLSs can be realized at the interface between the photonic lattices with a defect and the uniform photovoltaic-photorefractive (PP) crystals as well.

In this paper, we show that SDLSs are possible at the interface between the photonic lattices with a defect and the uniform PP crystals. These SDLSs exist in different bandgaps due to the change of defect strength. For a positive defect, SDLSs exist only in the semi-infinite gap and are stable in the high and low power regions but unstable in the moderate power region. For a negative defect, SDLSs exist in the semi-infinite and first gaps. In the semi-infinite gap, SDLSs are stable in the moderate power region but unstable in the high and low power regions. In the first gap, SDLSs are stable in the all power regions. On the other hand, the surface defect of photonic lattices can affect the properties of SDLSs. When the defect strength is increased, the stable region of SDLSs is extended for a positive defect and narrowed for a negative defect, and the power of SDLSs decreases with an increase in the positive defect strength and increases with the negative defect strength.

2. Theoretical model

Let us consider the physical situation in which an ordinarily polarized beam through a mask is launched into a PP crystal. The mask can control the distribution of optical intensity that forms the interface between the photonic lattices with a defect and the uniform PP crystal. Here such a defect resides in the interface. Meanwhile, an extraordinarily polarized probe beam is launched into the defect site, propagating along the interface with a defect. In this situation, the nondimensionalized equation for the probe

* Corresponding author.
E-mail address: kqlutj@126.com (K. Lu).

http://dx.doi.org/10.1016/j.optcom.2014.09.015
0030-4018/

beam is [15,17,36]

$$i\frac{\partial q}{\partial z}+\frac{\partial^2 q}{\partial x^2}+E_0\frac{I_L+|q|^2}{I_L+|q|^2+1}q=0. \quad (1)$$

Here q is the slowly varying amplitude of the probe beam, z is the normalized longitudinal coordinate (in units of $2kD^2/\pi^2$), x is the normalized transverse coordinate (in units of D/π), I_L is the intensity function of the photonic lattices described by

$$I_L=\begin{cases} I_0\ \cos^2(x)[1+\varepsilon g(x)], & x\geq -\pi/2 \\ 0, & x< -\pi/2 \end{cases}, \quad (2)$$

$E_0=k^2n_e^2r_{33}D^2E_p/\pi^2$, D is the lattice spacing, $k=2\pi n_e/\lambda$ is the optical wave number in the PP crystal, λ is the wavelength, n_e is the unperturbed extraordinary index of refraction, r_{33} is the electro-optic coefficient, E_p is the photovoltaic field constant, I_0 is the lattice peak intensity normalized by the dark irradiance I_d, $g(x)$ is a localized function describing the shape of the defect, and ε controls the strength of the defect. Such lattices described by Eq. (2) produce the interface with a defect inside PP crystals, which can support surface waves. At this point, we assume that the defect is restricted to a single lattice site at $x=0$. We choose function $g(x)$ as $g(x)=\exp(-x^8/128)$ and take $-1\leq\varepsilon\leq 1$. For a positive defect $\varepsilon>0$, the lattice light intensity I_L at the defect site is higher than that without defect. For a negative defect $\varepsilon<0$, the lattice intensity I_L at the defect site is lower than that without defect. For $\varepsilon=0$, the photonic lattices are uniform, as shown in Fig. 1(b). In this paper, let us consider a $BaTiO_3$ PP crystal with the following parameters n_e=2.365, $r_{33}=80\times 10^{-12}$ m/V, and $E_p=5$ KV/cm at a wavelength $\lambda=0.5$ μm. If $D=20$ μm, we find that $E_0\approx 8$ and that one x unit corresponds to 6.4 μm and one z unit corresponds to 2.4 mm in physical units.

In order to show the existent conditions for SDLSs, we look for Floquet-Bloch spectrum by substituting $q=f(x)\exp(ik_xx-i\mu z)$ into the linear version of Eq. (1) with ε=0, and obtain eigenfunction equation as follow

$$\frac{d^2f}{dx^2}+2ik_x\frac{df}{dx}-k_x^2f+E_0\frac{I_L}{1+I_L}f=-\mu f, \quad (3)$$

where $f(x)$ is the complex periodic function with the same periodicity as the lattices, k_x is wave number in the first Brillouin zone, and μ is the Bloch-wave propagation constant. We calculate Eq. (3) by the plane wave expansion method to obtain the bandgap diagram. Fig. 1(a) and (b) show the bandgap structure of the uniform photonic lattices when $I_0=3$ and the corresponding intensity distribution of the uniform photonic lattices, respectively. It reveals that there exist four complete gaps which are

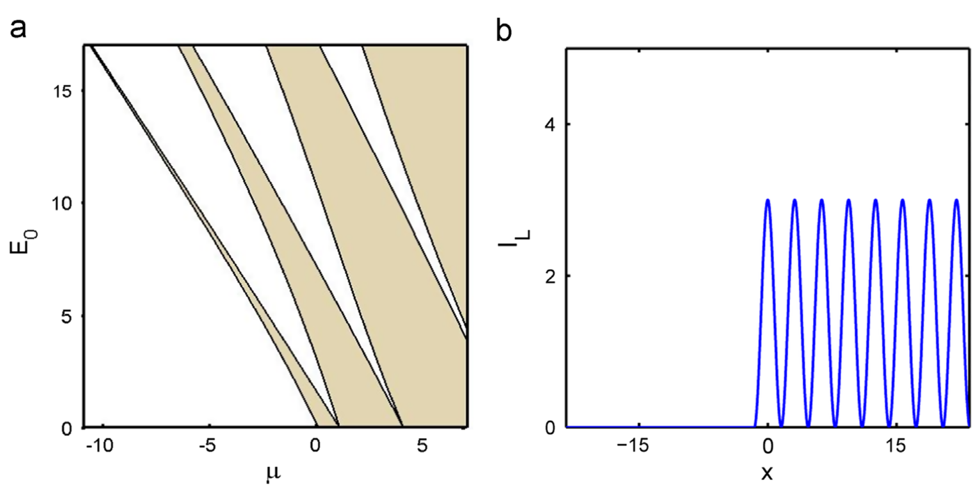

Fig. 1. (a) Photovoltaic field parameter E_0 versus the propagation constant μ; the shaded regions are Bloch bands. (b) Lattice intensity profiles with $I_0=3$ when $\varepsilon=0$.

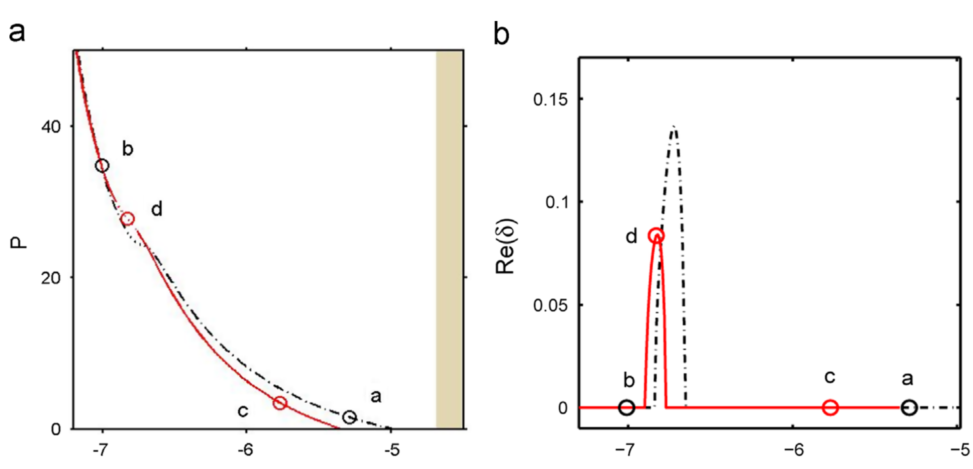

Fig. 2. (a) Power P versus propagation constant μ (shaded regions are Bloch band) at $I_0=3$ and $E_0=8$ when $\varepsilon=0.3$ (dash-dot curve) and 0.7 (solid curve). (b) Perturbation growth rates $Re(\delta)$ versus the propagation constant μ when $\varepsilon=0.3$ (dash-dot curve) and 0.7 (solid curve). In (a), the solid and dash-dot curves indicate the stable SDLSs, and the dotted curves indicate the unstable SDLSs, see (b). Profiles of SDLSs at the circled points in (a) and (b) are displayed in Fig. 3.